

Implementation of a multiple flow algorithm into the dynamic ecosystem model LPJ-GUESS

Jing Tang, Petter Pilesjö

Dept. of Physical Geography and Ecosystem Sciences
Lund University
Lund, Sweden
Jing.Tang@nateko.lu.se

Abdulghani Hasan

Department of Water Resources Engineering,
Duhok University
Duhok, Iraq

Abstract— The dynamic ecosystem model LPJ-GUESS includes explicit representation of vegetation dynamics as well as soil biogeochemistry, and has been widely and successfully implemented in predicting vegetation biomass and carbon cycling at different scales. However, the water cycling for each grid cell in the model is only considering the movement between atmosphere, vegetation and soil, ignoring the lateral water movement between grid cells. A previous study has proposed a distributed scheme in LPJ-GUESS incorporating topographic indices to redistribute lateral water movement, and has demonstrated the impacts on ecological functioning and carbon cycling at the Stordalen catchment, northern Sweden. The topographic indices, extracted based on a Digital Elevation Model (DEM), were based on a single flow (SF) algorithm at 50 m resolution, restricting the flow movement to the downslope cell with maximum gradient. In this study we have incorporated the Triangular Form-based Multiple Flow algorithm (TFM) to redistribute lateral water in LPJ-GUESS and analyzed the influences and differences between the two flow algorithms on runoff prediction as well as carbon cycling estimations. The results indicate that the runoff estimated by the TFM algorithm is more realistic than the SF algorithm. Besides, the comparison with observed runoff data demonstrates the monthly runoff estimated using the SF algorithm tends to overestimate the runoff in May and June as well as in the lower flatter peatland region. For the TFM algorithm, the underestimated runoff during the growing season can be compensated by the decreased soil depth in the elevated area. Moreover, the implementation of the TFM algorithm results in a significant increase of the catchment mean value of vegetation uptake of carbon as well as net ecosystem exchange carbon. We conclude that the advanced multiple flow algorithm (TFM) with more accurate estimation of flow accumulation can improve the hydrological predictions in LPJ-GUESS. Meanwhile, the results have proved that the flow routing algorithms do influence the vegetation pattern estimations for the study area.

INTRODUCTION

LPJ-GUESS is a dynamic ecosystem model, simulating vegetation dynamics as well as soil biogeochemistry [Sitch *et al.*, 2003; Smith *et al.*, 2001]. The model has been successfully implemented in predicting vegetation biomass, carbon balance, and carbon cycling at local and global scales [Ahlström *et al.*, 2012; Hickler *et al.*, 2004]. However, as an ecosystem model, the water cycling [Gerten *et al.*, 2004] is only limited to the interactions between atmosphere, plants and soil [Wolf, 2011]. There is no consideration of lateral water movement. A previous study proposed a distributed scheme by implementing topographic indices to add lateral water movement in LPJ-GUESS to conquer this limitation, and was renamed as LPJ-Distributed Hydrology (LPJ-DH) [Tang *et al.*, In Review]. The topographic indices, including drainage area (*DA*), flow direction (*Fdir*) and slope (*S*) are extracted from a Digital Elevation Model (DEM). Through applying *Fdir* to direct the generated runoff to downslope cells and using *DA* to organize the processing sequence, the new proposed LPJ-DH allows water flow between grid-cells, which is directly influencing the amount of vegetation available water as well as the runoff. The single flow algorithm (SF) [O'Callaghan and Mark, 1984] based on a gridded DEM was chosen for this application, assuming that surface flow only occurs in the steepest downslope direction.

The SF algorithm used in the previous study, in comparison to multiple flow algorithm (MF), restricts the divergence in estimating lateral flow paths [Hasan *et al.*, 2012; Zhou *et al.*, 2011] and therefore could influence the soil moisture and vegetation pattern estimations [Guentner *et al.*, 2004]. Many studies have suggested different methods of handling the multiple flows, and the majority work is based on gridded DEMs. However, due to the regularly spaced samplings on the continuous surface the gridded DEM could produce inconsistent flow paths [Zhou *et al.*, 2011], especially for coarser scales. To overcome the limitations of the gridded structure of the DEM, the newly-developed Triangular Form-based Multiple flow algorithm

(TFM) has been developed, based on the partition of grid cells into triangular facets and redistribution of water proportionally to down-hill adjacent cells [Pilesjö and Hasan, 2013]. In this way, the algorithm can better take into consideration the continuity using Triangulated Irregular Network (TIN). Besides, the improvements of flow routing over flat cells from the TFM algorithm was also evaluated [Hasan et al., 2012]. The TFM algorithm then showed the capability of producing the closest and consistent outcomes in relation to theoretical values of specific catchment area (SCA) compared to other methods.

In this paper the TFM algorithm is implemented to estimate topographic indices and adapt the distributed scheme in LPJ-DH to fulfill the divergence flow routing paths. Through comparing the hydrological and ecological estimations after coupling SF and TFM algorithm in LPJ-GUESS (named LPJ-DH-SF and LPJ-DH-TFM, respectively), we aim to answer the question how important the flow routing algorithms is in terms of modeled runoff and hydro-ecological variables at the catchment scale.

METHODS

The implementations of the SF and TFM algorithms are based on the same DEM, with the resolution of 50 m (to be consistent with the resolution of climate data). The main change in the LPJ-DH using the TFM algorithms is that the generated runoff can be directed to multiple downslope cells, instead of just one cell in the SF algorithm. So, the proportions of flow to downslope cells are added to each grid-cell as input attributes. Apart from that, in comparison with the single flow algorithm, the processing sequence of grid-cells for TFM cannot be uniquely determined by the values of DA alone, since some cells flowing to a downslope cell may have higher DA value. To overcome this problem, we found that implementing elevation (from higher to lower) together with DA values (from lower to higher) could uniquely decide the cell sequence for flow accumulation. A Matlab program was developed to test and make sure that the flow accumulation has been accomplished for the “upslope cells” before draining to “downslope cells”.

The sub-surface water routing is also included, and its lateral water redistribution follows the same principles as the surface water part. For the subsurface part, only vertical water movement is considered for unsaturated soil, and the saturated subsurface runoff ($R_{sub}(r,c)$) is estimated by quasi three-dimensional flow developed by Wigmosta et al. [1994]:

$$R_{sub}(r,c) = \frac{K_s}{f} [\exp(-fz_{wt}(i,j)) - \exp(-fD(i,j))] * S(i,j) * w$$

K_s is the saturated hydraulic conductivity varying with different soil types. $z_{wt}(i,j)$ is the distance from the ground surface to the water table (positive downward) and $D(i,j)$ is the total soil depth. f is the decay coefficient of saturated conductivity with depth and

w is the width of the flow. $S(i,j)$ is the slope of the cell. The parameter values of K_s and f are based on the literature.

The modeled runoff is compared with observed runoff measurements and evaluated by the relative root mean square error (RRMSE). The closer value of RRMSE to zero, the better is the model performance [Stehr et al., 2008]. To reveal the different flow algorithms influences on carbon fluxes, the Mann-Whitney U test was used.

$$RRMSE = \sqrt{\frac{\sum_{i=1}^n (S_i - O_i)^2}{n}} * \frac{1}{O}$$

STUDY AREA

Stordalen catchment

The Stodalen catchment is located in northern Sweden, about 9.5 km from the Abisko Research Station (ANS). The whole catchment covers 16 km² and consists of a mountainous area in the southern part, entering into the lower flat peatland area in the north (see Fig.1). The catchment hydrology has been reported by Persson et al. [2012] and Ryden et al. [1980] and water-related carbon fluxes measurements have been presented by Olefeldt et al. [2012] and Lundin et al. [2013]. For this study, measured daily runoff during the year 2007-2009 was provided by Olefeldt et al. [2012] in order to evaluate the model runoff estimations.

RESULTS

Drainage area

Presented in Fig.1, two different drainage patterns are estimated using the TFM (left) and the SF (right) algorithms. Through visual comparison, the TFM extracted drainage pattern shows smoother and more realistically looking spatial patterns than the SF estimated one. Additionally, the values of Ln(DA) from the SF algorithm are not smoothly increasing downhill, and the main drainage is more distinct.

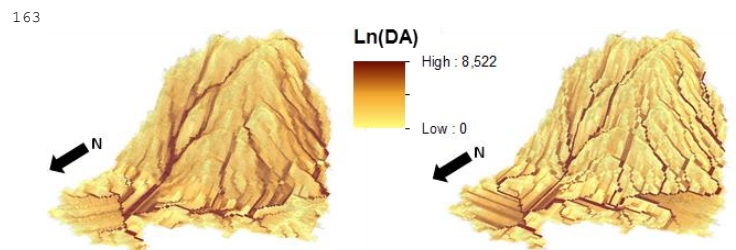


Figure 1. Map of Ln(DA) using the triangular form-based (left) and the single algorithm (right). For each grid-cell, the value 1 is added before calculating the natural logarithm. The map is draped on a digital elevation model (enhanced five times).

TABLE I. STATISTICS OF DRAINAGE AREA FROM TFM AND SF ALGORITHMS

Algorithms	Variables	Mean	Standard variation	Skew
SF	Drainage area(DA)	51.840	303.562	11.274
TFM	Drainage area(DA)	40.770	235.093	12.690

The results in Table 1 show that the TFM algorithm produces lower mean and variance values of DA and the higher and positive skew values indicate more cells with lower DA values when using the TFM algorithm. The allowances of flow divergence and consideration of consistency from the TFM algorithm reduce the DA average as well as the variances among cells.

Monthly runoff comparison

The daily runoff is summed up to get the monthly runoff, and the comparisons between observed and modeled runoff from LPJ-DH-SF and LPJ-DH-MF are presented in Fig. 2. The RRMSE values vary from point to point, but generally, the runoff peak from LPJ-DH-SF is higher than the LPJ-DH-MF, especially for the peatland cell A2. For the point A1, located at the catchment outlet, the LPJ-DH-SF produces lower RRMSE values, which capture the high runoff better in June during the observed years. For the point A2, the overestimation of runoff by LPJ-DH-SF is converse with the underestimation by LPJ-DH-MF during the summer period. For the point B2, with steeper terrain, both models are underestimating the runoff, but the LPJ-DH-SF shows values closer to the observed (RRMSE=4.14). For the relatively dry years (2008 and 2009), the runoff predictions at B2 have larger underestimation bias. For the outlet points A5 and A6, located in the comparatively flat region, both models show almost the same accuracy.

Going through the six measured points, for the LPJ-DH-MF the main discrepancy in runoff compared with observed data are the low runoff estimations in June. When the plants start to grow, there is more water supplying plants' photosynthesis and growth as well as soil evaporation, thus less water can route downslope. The distributed flow used in the TFM makes the available water to the main drainage network even less.

Carbon fluxes comparison

Due to lack of field data of spatially distributed biomass and carbon fluxes, the comparisons are based on the statistical comparison of models estimations over the whole catchment. The Mann Whitney U-tests indicate that the differences are significant for vegetation uptake carbon (VegCflux) and net ecosystem exchange (NEE) for the two models. The LPJ-DH-MF model has around 1.34% and 7.41% increase (more carbon uptake) in VegCflux and in NEE, compared with the LPJ-DH-SF outputs. There is no indication of significant difference of soil respired carbon (SoilCflux) between the two models. However, a distinctively higher soil released carbon can be found for the main drainage network cells from LPJ-DH-SF (see the whisker

extend for SoilCflux in Fig. 3), which is not appearing in LPJ-DH-MF.

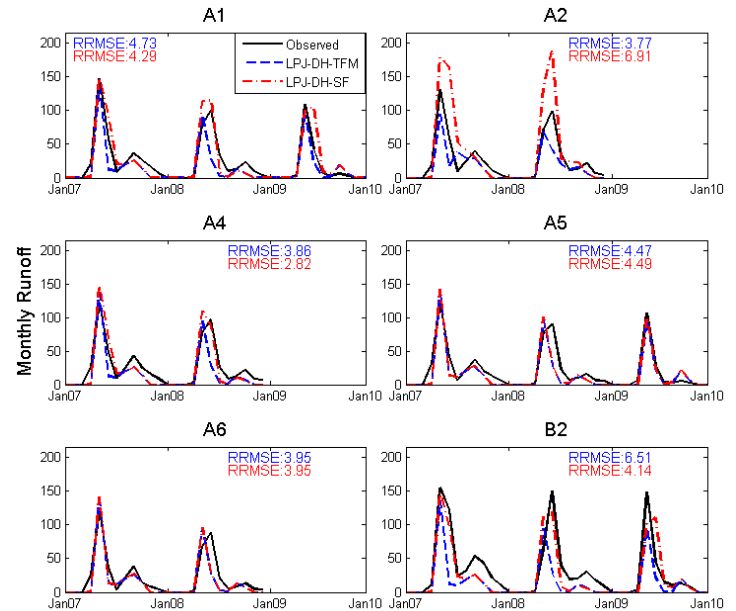


Figure 2. Point runoff comparisons between the modeled and the observed monthly runoff. There are no data for A2, A4 and A6 during the year 2009.

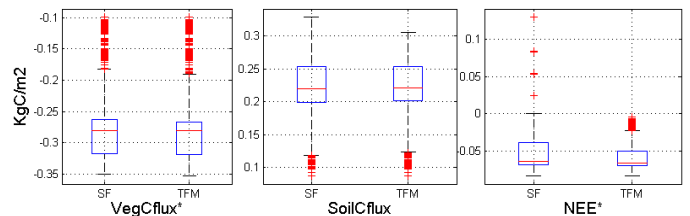


Figure 3. Catchment carbon fluxes diversity during the year 1981-2000. The asterisk (*) represents the statistical significance at the level of 0.05.

DISCUSSION AND CONCLUSION

In this study, the soil depth is set to 1.5 m, as the standard LPJ-GUESS depth, but in reality the soil is quite shallow with bare rocks in the southern mountainous area. The soil depth needs to be adjusted in forthcoming studies for the elevated area of the catchment. With reducing the soil depth, the runoff is expected to increase compared with the models outputs presented in this paper, but to what magnitude is unknown. The current results illustrate that the SF algorithm generally produces higher runoff values than the observed in May and June, with the exception of point B2. When reducing the soil depth in the southern elevated area, the runoff during the high-runoff season will become higher using the SF algorithm since the water is concentrated to the main flow paths. However, that could have less influence for the LPJ-DH-TFM due to the dispersion of water over the catchment

239 and maybe compensate the underestimated runoff for LPJ-DH- 290
240 TFM. 291
292

241 The allowance of flow divergence in the TFM makes the upslope 293
242 area per unit contour length decreasing [Wolock and McCabe Jr, 294
243 1995], which means there is less water accumulating for each 295
244 downslope neighboring cell. In other words, there are more cells 296
245 that could receive water from upslope cells which results in 297
246 significant changes in vegetation uptake carbon (total NPP) for 298
247 LPJ-DH-MF. With larger catchment and water-limited area, the 299
248 differences of flow routing on vegetation growth will be more 300
249 pronounced. 301
302
303
304

250 It is novel to evaluate two different routing algorithms by 305
251 implementing them into a process-based ecosystem model. In 306
252 this way, both the climate conditions and vegetation dynamics 307
253 are taken into the consideration. Comparing with other studies of 308
254 utilizing statistical correlations between topographic wetness 309
255 index (TWI) and vegetation pattern to evaluate different routing 310
256 algorithms [Kopecký and Čížková, 2010; Sorensen et al., 2006], 311
257 our method is more accurate and could reveal more detailed flow 312
258 algorithm differences/influences on hydrological estimations 313
259 through the seasons. Besides, our method can avoid using TWI as 314
260 a proxy for soil moisture conditions and can capture the effective 315
261 contributing area over time. Nevertheless, with increased 316
262 complexity of model structure, our method needs to be better 317
263 calibrated before finally concluding which routing algorithm that 318
264 is the best for different environments. 319
320
321
322

265 To summarize, the more advanced multiple flow algorithm 323
266 (TFM), producing more accurate estimations of flow 324
267 accumulation can improve the hydrological predictions in LPJ- 325
268 GUESS. The comparisons of carbon fluxes outputs between LPJ- 326
269 DH-SF and LPJ-DH-TFM have demonstrated that the flow 327
270 routing algorithms do matter not only for hydrological variables, 328
271 but also for ecological estimations, within the study area. 329
330
331

272 REFERENCES

273 [1] Ahlström, A., P. A. Miller, and B. Smith (2012), Too early to infer 333
274 a global NPP decline since 2000, *Geophys. Res. Lett.*, 39(15), L15403. 334
275 [2] Gerten, D., S. Schaphoff, U. Haberlandt, W. Lucht, and S. Sitch 335
276 (2004), Terrestrial vegetation and water balance—hydrological evaluation 336
277 of a dynamic global vegetation model, *Journal of Hydrology*, 286(1-4), 337
278 249-270. 338
279 [3] Guentner, A., J. Seibert, and S. Uhlenbrook (2004), Modeling 339
280 spatial patterns of saturated areas; an evaluation of different terrain indices, 340
281 *Water Resources Research*, 40(5). 341
282 [4] Hasan, A., P. Pilesjö, and A. Persson (2012), Drainage Area 342
283 Estimation in Practice - how to tackle artifacts in real world data, paper 343
284 presented at GIS Ostrava 2012-Surface models for geosciences, Ostrava, 344
285 Czech Republic. 345
286 [5] Hickler, T., B. Smith, M. T. Sykes, M. B. Davis, S. Sugita, and K. 346
287 Walker (2004), USING A GENERALIZED VEGETATION MODEL TO 346
288 SIMULATE VEGETATION DYNAMICS IN NORTHEASTERN USA, 346
289 *Ecology*, 85(2), 519-530.

[6] Kopecký, M., and Š. Čížková (2010), Using topographic wetness 347
index in vegetation ecology: does the algorithm matter?, *Applied 348
Vegetation Science*, 13(4), 450-459.

[7] Lundin, E. J., R. Giesler, A. Persson, M. S. Thompson, and J. 349
Karlsson (2013), Integrating carbon emissions from lakes and streams in a 350
subarctic catchment, *Journal of Geophysical Research: Biogeosciences*, 351
n/a-n/a.

[8] O'Callaghan, J. F., and D. M. Mark (1984), The extraction of 352
drainage networks from digital elevation data, *Computer Vision, Graphics, 353
& Image Processing*, 28(3), 323-344.

[9] Olefeldt, D., N. Roulet, R. Giesler, and A. Persson (2012), Total 354
waterborne carbon export and DOC composition from ten nested subarctic 355
peatland catchments—importance of peatland cover, groundwater 356
influence, and inter-annual variability of precipitation patterns, 357
Hydrological Processes, n/a-n/a.

[10] Persson, A., A. Hasan, J. Tang, and P. Pilesjö (2012), Modelling 358
Flow Routing in Permafrost Landscapes with TWI: An Evaluation against 359
Site-Specific Wetness Measurements, *Transactions in GIS*, 16(5), 701-713.

[11] Pilesjö, P., and A. Hasan (2013), A Triangular Form-based 360
Multiple Flow Algorithm to Estimate Overland flow Distribution and 361
Accumulation on a Digital Elevation Model, *Transactions in GIS*.

[12] Rydén, B. E., L. Fors, and L. Kostov (1980), Physical Properties of 362
the Tundra Soil-Water System at Stordalen, Abisko, *Ecological 363
Bulletins*(30), 27-54.

[13] Sitch, S., et al. (2003), Evaluation of ecosystem dynamics, plant 364
geography and terrestrial carbon cycling in the LPJ dynamic global 365
vegetation model, *Global Change Biology*, 9(2), 161-185.

[14] Smith, B., I. C. Prentice, and M. T. Sykes (2001), Representation of 366
vegetation dynamics in the modelling of terrestrial ecosystems: comparing 367
two contrasting approaches within European climate space, *Global 368
Ecology and Biogeography*, 10(6), 621-637.

[15] Sorensen, R., U. Zinko, and J. Seibert (2006), On the calculation of 369
the topographic wetness index; evaluation of different methods based on 370
field observations, *Hydrology and Earth System Sciences (HESS)*, 10(1), 371
101-112.

[16] Stehr, A., P. Debels, F. Romero, and H. Alcayaga (2008), 372
Hydrological modelling with SWAT under conditions of limited data 373
availability: evaluation of results from a Chilean case study, *Hydrological 374
Sciences Journal*, 53(3), 588-601.

[17] Tang, J., P. Pilesjö, P. Miller, A. Persson, Z. Yang, E. Hanna, and 375
T. V. Challaighan (In Review), Incorporating topographic indices into 376
dynamic ecosystem modeling using LPJ-GUESS, *Ecohydrology*.

[18] Wigmosta, M. S., L. W. Vail, and D. P. Lettenmaier (1994), A 377
distributed hydrology-vegetation model for complex terrain, *Water 378
Resources Research*, 30(6), 1665-1679.

[19] Wolf, A. (2011), Estimating the potential impact of vegetation on 379
the water cycle requires accurate soil water parameter estimation, 380
Ecological Modelling, 222(15), 2595-2605.

[20] Wolock, D. M., and G. J. McCabe Jr (1995), Comparison of single 381
and multiple flow direction algorithms for computing topographic 382
parameters in TOPMODEL, *Water Resources Research*, 31(5), 1315-1324.

[21] Zhou, Q., P. Pilesjö, and Y. Chen (2011), Estimating surface flow 383
paths on a digital elevation model using a triangular facet network, *Water 384
Resour. Res.*, 47(7), W07522.